

Received 9 December 2016; revised 4 February 2017; accepted 13 February 2017. Date of publication 20 February 2017; date of current version 24 April 2017. The review of this paper was arranged by Editor A. G. U. Perera.

Digital Object Identifier 10.1109/JEDS.2017.2671426

# ESC-DVS: Dynamic Voltage Scaling Using Entropy-Based Scene Change Detection for AMOLED Displays

BYUNG-HOON LEE AND YOUNG-JIN KIM (Member, IEEE)

Department of Electrical and Computer Engineering, Ajou University, Suwon 16499, South Korea

CORRESPONDING AUTHOR: Y.-J. KIM (e-mail: [youngkim@ajou.ac.kr](mailto:youngkim@ajou.ac.kr))

This work was supported in part by the National Research Foundation of Korea through the Korea Government (MSIP) under Grant 2015R1A2A2A01008434, and in part by Ajou University. This paper is an extension of an earlier version that appeared in the Proceedings of the 21st IEEE/ACM International Symposium on Low Power Electronics and Design in 2016 [41].

**ABSTRACT** Active matrix organic light emitting diode (AMOLED) displays are widely used in the displays of mobile devices. Whereas the display power accounts for a large portion of the total power of a mobile device, the computing power and battery size are limited. Thus, technologies for minimizing the computing overheads while reducing the power during video processing are important in mobile devices. In this paper, we propose a novel dynamic voltage scaling (DVS) method called ESC-DVS by designing low-overhead entropy-based scene change detection for video playback on mobile AMOLED displays. Its implementation using an MPEG4/H.264 player on an embedded board with a real mobile AMOLED display shows a power saving of 21.31% on average and higher accuracy compared to an existing power-saving scene change detection technique. In addition, the computing overhead decreases to 1/84 compared to an existing DVS technique while good human visual satisfaction is achieved.

**INDEX TERMS** AMOLED display, dynamic voltage scaling, scene change detection, videos, low power, entropy.

## I. INTRODUCTION

ACTIVE matrix organic light emitting diode (AMOLED) displays are mainly used on smartphones, such as the Samsung Galaxy S series, and are expected to be used more widely on diverse smartphone devices including the Apple iPhone [1]. In addition, the use of AMOLED displays has been increasing in large display systems such as monitors and TVs [2]. Whereas mobile devices have shown more diverse functions as time has passed, the battery capacity technologies have not maintained the same pace. Therefore, power-saving technologies for mobile devices are very important. One of the components of a mobile device that consumes the largest amount of power is the display panel [2]. Therefore, studies on reducing the power consumption on diverse panels have been actively conducted [3]–[5].

One of the major applications on a display panel is video playback. In Fig. 1, the proportions of video app usages on mobile devices such as tablets and smartphones are high. Videos are also widely used in social networks

messages as well as TV and movies [6]. Owing to the exponential increase in video content, watching all available videos is impossible. Therefore, the need for functions allowing users to search and view only those scenes that are important to them is increasing. Accordingly, a number of attempts have been made to allow all meaningful information to be extracted from video sequences [7]. Scene change detection, which is one of the many video segmentation techniques available, is a structural approach to obtaining video information. A lot of scene change detection studies have recently combined pieces of video information into frames in order to segment, and thereby hierarchically analyze the information [8]–[14].

Scene change effects can be divided into abrupt and gradual scene changes. Abrupt scene changes can be relatively easily detected because the boundary frames and previous frames are clearly different. Gradual scene changes are relatively difficult to detect because the same characteristics as in abrupt scene changes appear across many frames, and thus the scene change points cannot be clearly

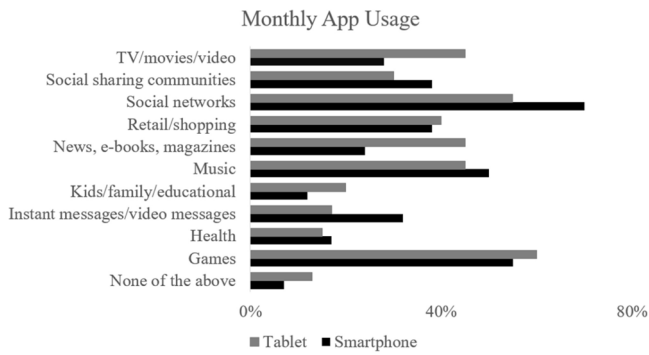


FIGURE 1. Monthly app usages of tablets and smartphones [6].

determined. Representative gradual scene change effects include fade-in, fade-out, dissolve, and wipe effects, which can be divided more minutely depending on the type of film-editing techniques applied.

The most basic method for reducing power consumption in AMOLED displays is lowering the voltage supplied to the panel. Because a distortion in quality occurs in a video content when the voltage is scaled, different degrees of quality control based on the supply voltage level are very important. A method for flexibly determining the supply voltage based on such degrees of quality control through the supply voltage level is called a dynamic voltage scaling (DVS) technique. AMOLED displays consist of R, G, and B sub-pixels, and their power consumption varies based on the composition of the sub-pixels displayed on the panel owing to their self-luminous characteristic. Therefore, DVS techniques that can maximize the power-saving depending on the content while minimizing the quality distortion are sorely needed. Among existing DVS studies, those minimizing the distortion of still images on passive matrix OLEDs (PMOLEDs) are representative [15]. In addition, studies have applied voltage-scaling simulations using scene change detection that evenly divides the AMOLED display panels and calculates the differences in pixels between frames [16].

In the meanwhile, power saving schemes have been actively researched for OLED displays in recent years. Lin *et al.* [17] modeled the image scaling optimization problem that minimizes power while preserving image quality. Chen *et al.* [18], classified images using Hidden Markov Model (HMM) classifiers and then proposed a dynamic tone mapping method to improve power efficiency while controlling display quality. Chang and Xu [19] proposed a method to convert RGB values of an image dynamically and in real time based on PSNR, thereby saving power consumption. Kim *et al.* [20] focused on the fact that the power efficiency of each pixel of the OLED display is different, and power saving was achieved through color conversion while maintaining image quality.

In this paper, we propose a novel DVS technique using entropy-based scene change detection for mobile AMOLED displays. To detect a scene change in favor of low power, we

first propose a novel scene change detection method called ESC, which contains the calculation and comparison of the entropies of Y, Cb, and Cr components in the YCbCr color space. ESC enables scene change detection with more correctness and less overhead for high power saving. Also, it minimizes required operations by using information from macroblocks in the decoding process. Then, we propose an ESC-based DVS method (ESC-DVS), which improves the video quality better by compensating Y, Cb, and Cr components after voltage scaling in comparison with gray level pixel compensation. To consider the limited resource environment of the mobile device, we use three lookup tables for a real AMOLED display-based board.

The remainder of this paper is composed as follows. In Section II, studies regarding scene change detection techniques and power saving for AMOLED displays are introduced. In Section III, the contributions and motivation of this study are described. In Sections IV and V, new scene change detection and voltage-scaling techniques are introduced, respectively. In Section VI, strategies for reducing the operational overhead are described. In Section VII, the experiment environment and results using the proposed algorithm are described. In Section VIII, a discussion on the findings of this research is provided, and finally, in Section IX, some concluding remarks are given.

## II. RELATED WORK

### A. SCENE CHANGE DETECTION TECHNIQUE

Videos are stored in compressed formats and are displayed by decompressing the compressed files. A scene change detection method applied to a compressed video file selectively decodes the bit strings and applies a detection algorithm with the proper decoding information [8]. This is based on the advantage in that, when video segmentation has been applied in a compressed state, the computing overhead and storage capacity can be reduced. However, because the macroblock sizes may be diversely changed according to the panel resolution and the number of codecs, and are affected by the reference frame, this method cannot be used directly. In addition, classification methods using a motion vector have limitations in expressing entire changes because motion vectors express only local changes in a narrow sense within the frame [9].

Because videos are expressed as pixels on a display panel, studies directly using the pixel information are the most common. In addition, because it is difficult to understand the characteristics of individual frames based on the pixel information, the difference in pixel values between frames and the pixel histogram information are used [10], [11]. However, this method has a shortcoming in that it cannot respond to an overload because, as the resolution of a video increases, the number of operations that must be processed per frame also increases. In addition, this method has an additional shortcoming in that the movements of an object within the same scene cannot be accurately detected based solely on the changes in pixels. Studies intending to supplement these

shortcomings include separately extracting the backgrounds from individual frames and estimating an object's movements using the differences between the backgrounds [12].

Compared to studies focusing on pixel information, many studies conducted on scene change detection have resulted in a relatively smaller computing overhead. Among them include studies by Cemekova *et al.* [13] and Baber *et al.* [14], who applied the theory of entropy values as information functions. Cemekova *et al.* [13] showed that cuts and fades, which are scene change effects, are detectable through the joint entropy between one frame and the previous frame, and the amount of mutual information between them. Baber *et al.* [14] calculated the entropy values while analyzing the relevance of speeded up robust features (SURF) based on the gray levels of successive frames to detect frames in which the scenes are changed. However, because this method uses only the gray levels, it is vulnerable to color-difference centered scene change effects, such as dissolves. In addition, when all pixels present between frames are processed, an excessive computing overhead is required, which is undesirable for mobile environments. To achieve power saving in embedded boards with limited resources, such as mobile devices, scene change detection techniques based on a dramatically low overhead are needed.

Videos include group of picture (GOP) information, which is a set of video frames for MPEG video compression. There are three kinds of representative frame types in GOP; I-, P-, and B-frames. I-frames are those in which the input signals are stored as they are without the use of any predictions or data for compositing a complete image. P-frames contain only predictive information made by observing the differences between the current frame and the previous I-frame. Because these frames contain only predictive information, unlike I-frames, they contain less data than I-frames. B-frames are two-way prediction frames composed by evaluating the differences between the previous frame and the next frame. B-frames use less data than P-frames, and similar to P-frames do not show the original video. Taking note of these structures, studies have been conducted that apply a power-saving algorithm each time an I-frame composes a complete frame when the video is played back [21], [22]. However, because I-frames are determined regardless of the video content, owing to the recent developments in compression technology, optimum power saving is difficult to achieve in many cases. In addition, existing studies have focused on CPU power saving.

### **B. LOW POWER AMOLED DISPLAY TECHNIQUE**

Shin *et al.* [15] applied DVS to still images for PMOLED displays, which are a type of OLED. This study was intended to adjust the voltage supplied to the panel while reducing the amount of distortion through a compensation scheme that restores the luminance based on the decreased voltage. However, because this technique involves a large computing overhead owing to the repeated calculations of the optimum

video distortion while reducing the supply voltage, this technique is not suitable for application to videos with a high resolution or for embedded devices with limited resources. In addition, this technique compensates only the gray-level distortion of the color differences compared to the original video. Finally, the PMOLED display used by the authors in their experiments has been used in very limited cases such as sub-displays owing to its simultaneous light emission by an entire line of pixels.

Chen *et al.* [16] proposed a DVS technique using pixel-difference based scene change detection for AMOLED displays. This technique was intended to continuously maintain the video quality while saving power. However, this technique has a shortcoming in that the computing overhead is large owing to the measurement and evaluation of the pixel similarity between frames during the scene change detection. In addition, because this study conducted simulation-based experiments, the environments of actual embedded boards were not considered.

When dynamic voltage scaling is applied, the magnitude of the voltage supplied to the panel changes, and accordingly, the luminance of the video displayed on the panel also differs from the original. Therefore, color compensation studies for recovery from luminance changes following voltage scaling have been actively implemented. Ku and Wang [23] proposed adaptive luminance changes based on the relationship between the YCbCr color space luminance information and the maximum color difference vector. However, this technique has a problem in that it leads to an over color saturation compared to luminance changes because the luminance and saturation are adjusted separately. Chiang *et al.* [24] considered the relationships among luminance, saturation, and hue to achieve higher human visual satisfaction. However, their study has a problem in reflecting the characteristics of the panel used because it was also conducted through simulations. Park and Song [25] added an 8-bit operation for power saving through alpha blending. However, this study has a shortcoming of abrupt increases in computing overhead. These studies are therefore not suitable for mobile devices with limited resources because the studies utilize the memory inefficiently.

### **III. MOTIVATIONS AND CONTRIBUTIONS**

Among the different DVS studies conducted on video playback for AMOLED displays, the method proposed by Chen *et al.* [16] is representative. However, we observed through MATLAB-based experiments that this method has the following problems.

1. The technique divides a single frame into 16 regions, calculates the pixel differences from the previous frame based on region, and identifies non-similar regions based on the degrees of pixel changes. If a frame has eight or more non-similar regions, that is, one-half or more of the regions, a scene change is detected to have occurred. This technique has a shortcoming in that its accuracy will be reduced considerably when the pixel changes continuously exceed the

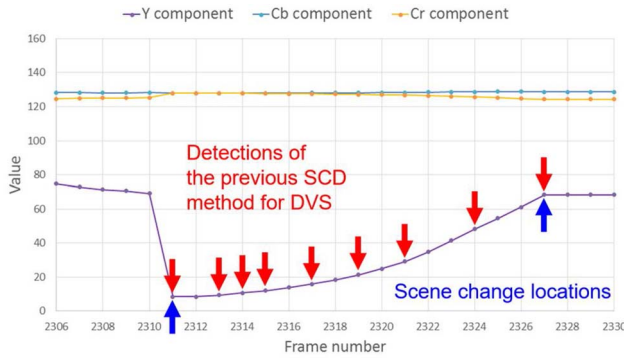


FIGURE 2. Y, Cb, and Cr components in 'fade in'.

detection criteria owing to a pixel difference between a frame and its previous frame.

Fig. 2 shows the detection results of the technique proposed in [16] for a fade-in, which is a gradual scene change effect. As the video progresses from frame 2,310 to frame 2,311, an abrupt scene change occurs. Thereafter, a fade-in effect progresses from frame 2,311 to frame 2,327. During this process, a larger number of scene detections occur than the number of times the scene actually changes. Unnecessary scene detections lead to increases in unnecessary computing overhead such as unnecessary supply voltage adjustments. In addition, this technique involves a shortcoming in that the quality of the video deteriorates as the luminance changes regardless of the video flow following the changes in voltage within the same scene.

2. Instead of being conducted on actual panels, the experiments were conducted through simulations. Unlike a desktop environment, a mobile environment has limited power sources and generally demonstrates a lower computing performance. For actual operation in such environments, techniques requiring little computing overhead are necessary.

Because most existing scene change detection techniques have focused solely on precise scene detection [8]–[14], they are not suitable for use on mobile devices with limited power and resources. Existing scene change detection techniques for DVS [16] are weak in terms of gradual scene change detection and have a shortcoming in that they have not been implemented on actual display boards but rather have been experimented through simulations. In addition, most existing DVS techniques that include compensation techniques are not suitable for video playback because their computing overheads are large. Furthermore, because they compensate only the gray level, they involve a distortion of the color difference information. The contributions of this paper can be described as follows.

1. We propose a power-aware scene change detection method with high accuracy compared to existing techniques. The proposed method uses the characteristics of entropy change in each frame when the video is played.

2. We propose a scene change detection method with less overhead than existing techniques. In the proposed method, the amount of computation is reduced by using YCbCr information of the macroblocks in the decoding process rather than using the RGB information in the buffer before the display output.

3. We propose a dynamic voltage scaling method that guarantees improved quality. Unlike the existing techniques which only compensate the gray level, the proposed method enhances the quality by carrying out color difference compensation.

4. We implement the proposed method for an MPEG4/H.264 player on a board with an AMOLED display panel. This is because the method considers the limited computing performance and battery capacity in mobile device.

#### IV. ENTROPY-BASED SCENE CHANGE DETECTION

Video frames are composed of numerous scenes. Scenes can be defined as sets of frames with coinciding objects and backgrounds. In this paper, boundary frames between every two scenes are detected with an aim to maintaining the same quality as the original video while reducing the power consumption through supply voltage control. For DVS, only video luminance information should be considered. However, taking note of the fact that the amounts of power consumed by individual sub-pixels differ because of the characteristics of the AMOLED displays, a more accurate scene change detection method using Cb and Cr information is proposed herein. In this way, even when the voltage is not scaled, more optimized compensation for the content can be implemented at the scene boundary points where the luminance levels are similar, and the power consumption can be slightly reduced.

##### A. YCBCR COLOR SPACE

The colors displayed on a display panel are expressed as an RGB color space. However, if an entire video is stored as RGB, the video size will be quite large. Therefore, the YCbCr color space is used to efficiently compress the video for storage. In the YCbCr color space, Y refers to the luminance, Cb refers to the difference vector between the luminance and blue color, and Cr refers to the difference vector between the luminance and red color. Conversion between the YCbCr and RGB color spaces follows Eq. (1) [26].

$$\begin{bmatrix} Y \\ Cb \\ Cr \end{bmatrix} = \begin{bmatrix} 16 \\ 128 \\ 128 \end{bmatrix} + \begin{bmatrix} 0.257 & 0.504 & 0.098 \\ -0.148 & -0.291 & 0.439 \\ 0.439 & -0.368 & -0.071 \end{bmatrix} \begin{bmatrix} R \\ G \\ B \end{bmatrix}. \quad (1)$$

##### B. ENTROPY THEORY

Entropy values are used to remove redundancy during the encoding/decoding of a video. In contrast, the video entropy values express the pixel distribution. Only gray-level entropy information is used, which creates certain limitations in terms of scene detection. To supplement the low accuracy of scene



change detection in scenes with similar colors between an object and the background, the proposed technique uses Cb and Cr entropy values that include the color difference information. Entropy values are used as a tool to measure the uncertainty of a random variable while being used as an information function, as indicated through Eq. (2).

$$E_X = \sum_{y \in A_x} P_y \log \frac{1}{P_y} \quad (2)$$

Entropy values as an information function refer to dataset information measurement methods. That is, entropy values are defined as the expected values of information. Individual information increases when the probability is lower. Larger numbers of values with low probabilities mean that the number of cases that may occur is larger, thereby leading to an increase in entropy.

In video processing, entropy includes information on diverse pixel values. The entropy decreases as the ratio of single pixels that constitute a video increases. On the contrary, the entropy is smaller for a video composed of more diverse pixels [14]. Even when the average luminance levels of different sequences of video information output on a display panel are the same, the scenes may be expressed differently depending on the distribution of the luminance levels. For instance, Y may be uniformly 100 for all pixels, or may be 50 for half of the pixels and 150 for the remaining half. In addition, there may be other diverse cases in which the average value of Y is 100. That is, the entropy values vary with diverse cases, and scene change detection is implemented based on these characteristics.

### C. SCENE CHANGE EFFECTS

Scene changes are divided into gradual and abrupt scene changes. Abrupt scene changes refer to changes from one scene to another without any transition effects. Because there are clear differences between scenes, abrupt scene changes can be relatively easily detected. These differences can be detected by identifying large changes in the entropy of the Y, Cb, and Cr components of the macroblocks in each frame. The change between frame 2,310 and frame 2,311 in Fig. 2 is an abrupt scene change.

Gradual scene changes are transition effects used by an editor to provide a dramatic effect to the viewers when one scene is changed into another. Representative scene change effects include fade-in, fade-out, and dissolve. Dissolve effects refer to a scene change technique in which a scene gradually appears while the previous scene gradually disappears. Fade-in and fade-out effects refer to effects in which a dark scene become gradually bright or a bright scene becomes gradually dark as the scene changes. Scene change effects applied to many different frames may cause abrupt entropy changes, and when such effects have terminated, the entropy maintains a constant value. In this paper, such a point is called a change point, which means the point at which the tendency of the cumulative variables of the Y, Cb,

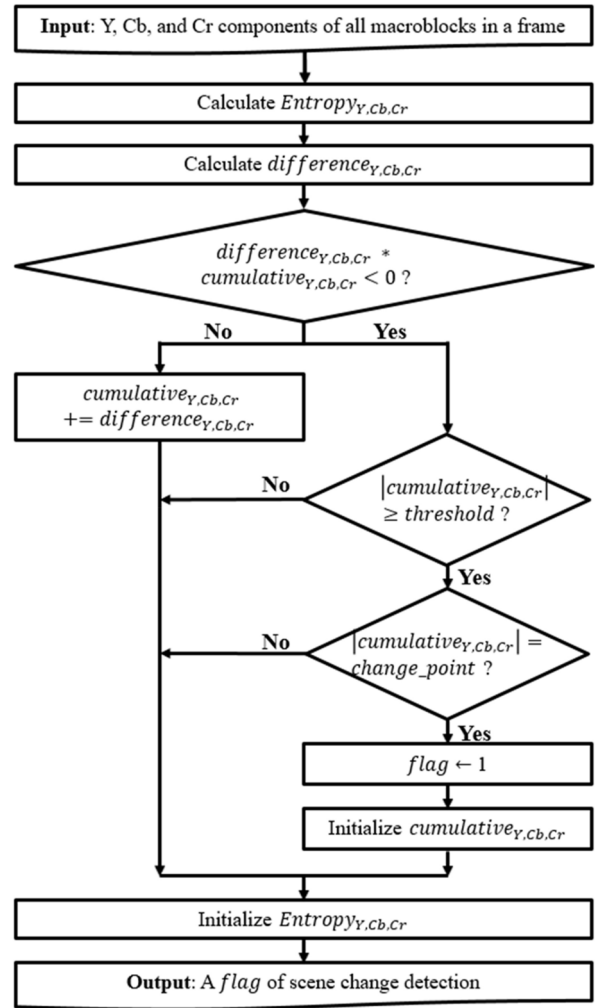


FIGURE 3. Flow of the ESC algorithm.

TABLE 1. Variables used in the ESC algorithm.

Variables	Meaning
$entropy_{Y,Cb,Cr}$	Entropy of Y, Cb, and Cr components of all macroblocks in the frame
$difference_{Y,Cb,Cr}$	Difference entropy of Y, Cb, and Cr components of the previous frame and the current frame
$cumulative_{Y,Cb,Cr}$	Cumulative variables of difference entropy until a scene change is detected
$threshold$	Entropy variation for scene change detection
$change\_point$	The point at which the tendency of cumulative variables changes from an increasing tendency to a decreasing tendency, or vice versa.
$flag$	Variable for detecting a scene change

or Cr component in the YCbCr color space changes from an increasing tendency to a decreasing tendency, or vice versa.

### D. ESC ALGORITHM

Fig. 3 shows the entropy-based scene change detection (ESC) technique proposed in this paper. Table 1 shows the variables used to describe the ESC technique in Fig. 3. The ESC algorithm is largely composed of the calculation and comparison of the entropy values of the Y, Cb, and Cr components

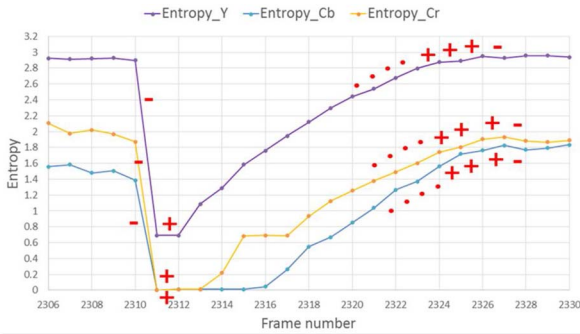


FIGURE 4. Entropy of Y, Cb, and Cr components in ‘fade in’.

of the macroblocks in each frame. First, when a video is played, whether the scene has changed is detected in the first frame. Thereafter, the entropy in the frame is calculated. Once the first frame has been completely output, the second frame progresses. After calculating the entropy of the second frame, the entropy is compared with that of the first frame. The difference in the entropy values between the current frame and the previous frame is calculated, whether the scene has changed is then detected using the result, and the cumulative entropy is calculated. The cumulative entropy is calculated to see the amount of change in entropy between the scene boundary frame and the current frame. Through the cumulative entropy and the sign of the entropy difference, the luminance of the video and how the color difference information is changed can be determined. If the cumulative entropy value is larger than the threshold and has reached the change point, the scene is determined to have been changed at that point. In this case, the conditions in which the change point has been reached, and the value of the cumulative variable is larger than the threshold value, should be satisfied by all three components: Y, Cb, and Cr. When the scene change detection has been made, the supply voltage is set according to the boundary frame information. Using the ESC algorithm, the threshold value was set to 0.2 based on experiments with many videos of various types.

### E. EXAMPLES OF THE ESC ALGORITHM

Fig. 4 and 5 describe the process used to apply the ESC algorithm to scene change effects, where the video applied is the same as that shown in Fig. 2. Fig. 4 and 5 show the entropy change points and the video points by frame, respectively. The horizontal axis in Fig. 4 indicates the frames, and the vertical axis indicates the entropy values. This figure shows changes in the entropy values of the individual Y, Cb, and Cr components as graphs according to the frame progression. From frame 2,310 to frame 2,327, a scene change effect, i.e., a fade-in, is progressing. Because this effect is a transition effect for a dark scene to slowly become bright, the entropy values of the individual components increase as the frames progress. As explained through Fig. 3, as the frames progress,

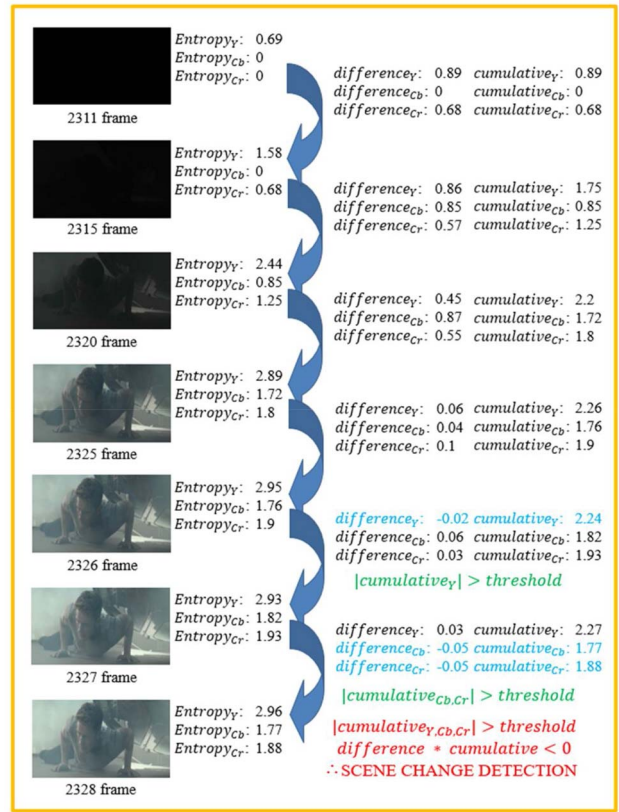


FIGURE 5. Example application of the ESC algorithm.

the entropy differences and cumulative variables are calculated, and when the values of the cumulative variables have exceeded the threshold and have reached the change point, a scene change is detected. Concrete values in scene change detection are described in Fig. 5 along with the actual frame images.

Fig. 5 shows the application of the ESC algorithm based on the actual values of the actual entropy-related variables together with the frame images. As the frames progress, the entropy values of Y, Cb, and Cr increase, as do the difference and cumulative variables. Based on frame 2,311, where an abrupt scene change has occurred, the value of a cumulative variable, which is one of scene change detection criteria, exceeds the threshold value from frame 2,317. Thereafter, the second criterion, the change point, is checked. Because the entropy value of the Y component decreases from that of the previous frame as the video progresses from frame 2,326 to frame 2,327, this point becomes a candidate for scene change detection.

The detection is postponed to a later time, however, because the cumulative variables of the Cb and Cr components show an increasing trend. When the video progresses to frame 2,328, because it can be seen that this point is a change point owing to the decrease in the entropy values of Cb and Cr, and thus the sign of the difference values is changed and the value of the cumulative variable becomes

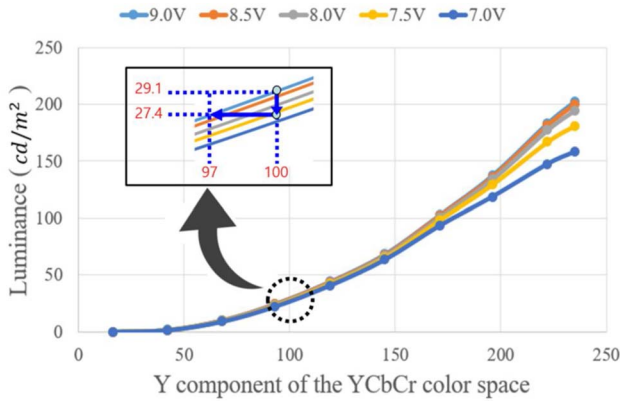


FIGURE 6. Luminance vs. Y component.

larger than the threshold value, the ESC algorithm determines that a scene change has occurred.

## V. ESC-DVS ALGORITHM

### A. LUMINANCE AND Y COMPONENT

DVS is a technique for actively controlling the supply voltage, and a minimization of the quality distortion from the voltage scaling is important. To maintain the quality while reducing the power consumption, the amount of change in luminance during voltage scaling is considered herein. This is based on the theory indicating that the HVS is more sensitive to changes in luminance than changes in colors [27]. Fig. 6 shows the relationship between the luminance levels based on the supply voltage and the Y component in the YCbCr color space on a CHIMEI C0240QGLA-T display panel [28]. Here, the maximum supply voltage was 9.0 V, and the minimum supply voltage was 7.0 V. In addition, because the video was at the gray level in the RGB color space, the values of the Cb and Cr components were fixed to 128.

The loss of luminance increases as the voltage supplied to the panel is reduced. Therefore, the just noticeable difference (JND) [29] is used to avoid damaging the video quality. JND refers to cases in which the Euclidean distance between two colors is within 2.3 in the CIE Lab color space, because it is known that the HVS cannot detect the difference in such cases. The Euclidean distance measurement formula is shown in Eq. (3).

$$\Delta E_{ab}^* = \sqrt{(L_2^* - L_1^*)^2 + (a_2^* - a_1^*)^2 + (b_2^* - b_1^*)^2} \quad (3)$$

For instance, if the voltage is scaled down from 9 to 7.5 V, as shown in Fig. 6, the luminance value will be changed from 29.1 to 27.4. Here, 27.4 is the luminance value when the Y component is 97 at 9 V. If this change in Y component is expressed as a Euclidean distance, it will be 1.65, which can be said to satisfy the JND. Using this method, the DVS technique proposed in this paper was composed such that the voltage can be dynamically changed according to the content

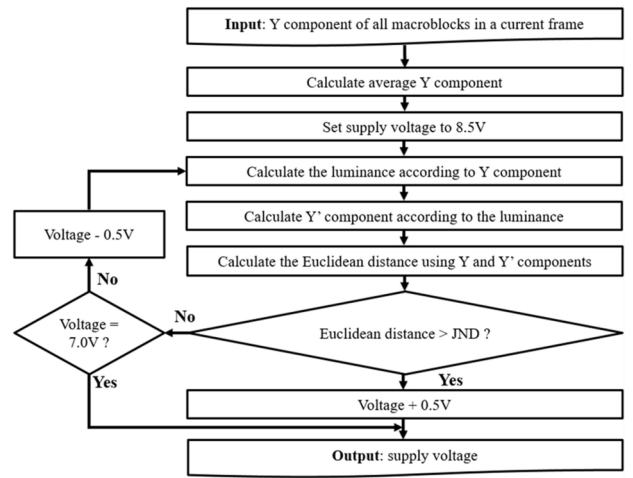


FIGURE 7. Determination of a supply voltage according to Y component in a scene boundary frame.

information during video playback based on changes in the Y component depending on the voltage.

### B. DVS ALGORITHM

#### B.1. SUPPLY VOLTAGE DETERMINATION

Fig. 7 shows the proposed DVS algorithm, which operates based on the relationship between the luminance and Y component, as shown in Fig. 6. First, the Y components of the macroblocks in the current frame are received as inputs. The average Y values for the individual Y components in the current frame are then calculated. Thereafter, the current supply voltage is set to 8.5 V, which is one level lower than the maximum voltage. The luminance value of the frame is next calculated based on the current supply voltage, and the value of Y' according to this luminance value is calculated based on the relationship shown in Fig. 6.

Using Eq. (3), the Euclidean distances for Y and Y' are calculated. In this case, because Y and Y' indicate the gray level, Cb and Cr are both fixed at 128. The calculated Euclidean distances are compared to the JND, which is again 2.3. This calculation is repeated until the Euclidean distance shows the largest value not exceeding 2.3. In addition, if the supply voltage is lower than 7.0 V, the Euclidean distance calculation should be stopped, and 7.0 V should be output as the supply voltage because the voltage cannot be reduced to below 7.0 V owing to the characteristics of the hardware used in the present study. In the case of actual video playback, this process is implemented offline for faster operation processing. When conducting experiments on a real board, the supply voltage scaling process was implemented using separate functions, allowing the supply voltage to be determined according to the Y component of the current frame.

#### B.2. Y COMPENSATION

Fig. 8 shows the Y compensation algorithm according to the supply voltage scaling, as shown in Fig. 7. When the supply

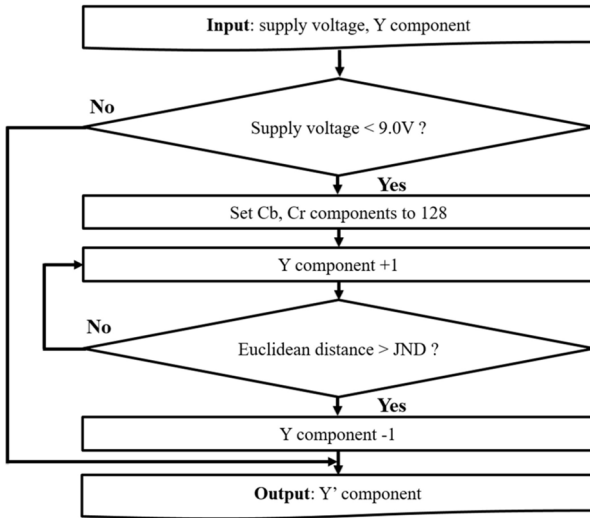


FIGURE 8. Y component compensation algorithm.

voltage is reduced, the panel luminance is also reduced. Because this means a distortion in the video quality, compensation to recover such distortion is necessary. Among the Y, Cb, and Cr components, because the Y component directly affects the luminance, Y component compensation is applied first. Such application is provided for the Y components of the individual macroblocks. The algorithm for this, shown in Fig. 8, is as follows.

The scaled supply voltage and the original Y are received as inputs. Whether the supply voltage is 9.0 V, which is the maximum supply voltage of the hardware used in this paper, is determined. If it is the maximum supply voltage, the original Y is output as is because the original video should not have been distorted. If the supply voltage is not the maximum voltage, the values of Cb and Cr are fixed at 128 to calculate the Euclidean distance based on the gray level. The Y value is increased by 1, the Euclidean distance between the increased Y and the original Y is calculated, and the result is compared with the JND. The maximum value of the increased Y is obtained when the Euclidean distance does not exceed the JND, and the compensated Y (i.e., Y') is output. As shown in Fig. 8, the process used to obtain the maximum value with the Euclidean distance not exceeding the JND is composed as lookup table 1 (LUT 1) through an offline operation with an aim to reduce the computing overhead for seamless real-time video playback.

### B.3. Cb, Cr COMPENSATION FOR ADDITIONAL POWER SAVING AND HIGH VIDEO QUALITY

AMOLED display power models are often expressed as shown in Eq. (4) [30].

$$P_{AMOLED} = C + \sum_{i=1}^n \{f(R_i) + h(G_i) + k(B_i)\} \quad (4)$$

As can be seen in the equation, the relationships among the power consumption and the R, G, and B components

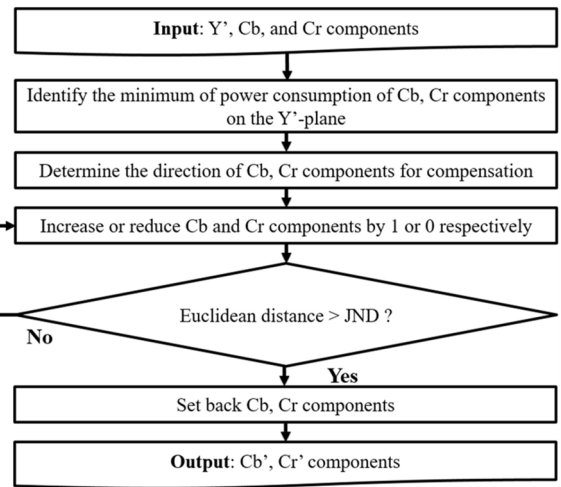


FIGURE 9. Cb, Cr compensation algorithm.

in the RGB color space are linear, where the power consumption increases as the R, G, or B component increases. However, because compensation is implemented in the YCbCr color space in this paper, linear compensation cannot be implemented based on Eq. (4). Therefore, a process for calculating the minimum point at which the power consumption can be minimized is necessary, which is explained in detail in Section VI. Compensation for the color differences is achieved by obtaining the maximum value when the Euclidean distance of Cb and Cr does not exceed the JND, similar to the Y component compensation method. The Euclidean distances are calculated based on the Y value equal to Y', which is the output shown in Fig. 8.

Fig. 9 shows a Cb, Cr component compensation method, which operates as follows. The value of Y', which is the output shown in Fig. 8, and the Cb, Cr information of the individual macroblocks of the current frame are obtained as inputs. The points where the Cb, Cr power consumption values are minimum on the Y'-plane are identified, and whether to increase or reduce the Cb and Cr values is determined independently based on the results. The Cb and Cr values are increased or reduced by 1 or zero, respectively, and the Euclidean distance between the calculated Cb', Cr' and Y' values received as input is determined.

The maximum values of Cb', Cr' when the Euclidean distance does not exceed the JND are obtained, and the maximum Cb', Cr' values are applied as output when the current frame is output on the panel. Because the overhead for the method shown in Fig. 9 is too large to apply in real-time during actual video playback, the processes for determining the direction and amount of compensation are converted into two lookup tables called LUT 2 and LUT 3, respectively, which are used separately during an offline operation.

### B.4. ESC-DVS ALGORITHM

Fig. 10 shows the entire ESC-DVS algorithm proposed in this paper. If scene changes are detected by applying the



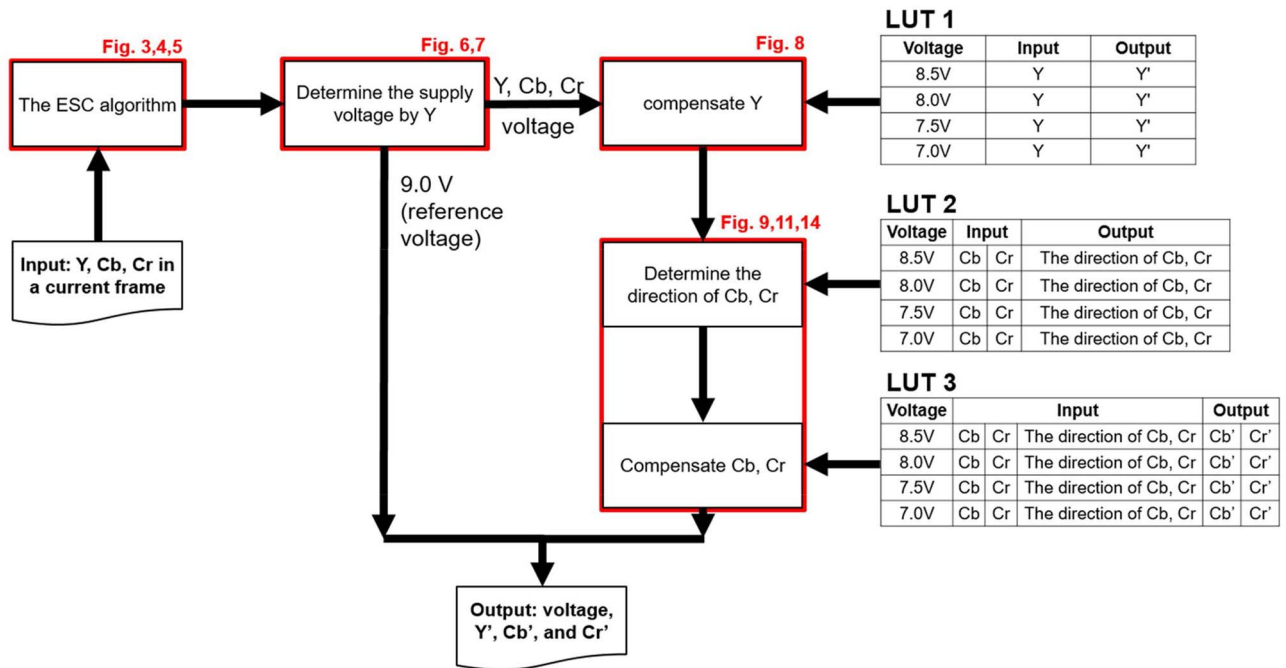


FIGURE 10. Block diagram of the ESC-DVS algorithm.

ESC algorithm, the voltage is scaled to the level that can maximally reduce the power consumption within the range of the JND. If the current frame belongs to the same scene as that of the previous frame, the same voltage as that of the previous frame is maintained. If the supply voltage is not the maximum voltage of 9 V, the luminance will change following the voltage scaling, and a compensation process should be implemented to recover the luminance. In this case, the direction of compensation is determined to minimize the power consumption based on the JND. Concretely, the Y component is compensated first based on the scaled voltage. Thereafter, to compensate the differences in color, whether Cb and Cr should be increased or reduced is determined because, unlike the RGB color space, the individual components and their power consumption are not proportional to each other in the YCbCr color space. When the directions of the Cb and Cr compensation have been determined, Cb and Cr are compensated within the range in which the Euclidean distance does not exceed the JND. Lookup tables are used during the compensation process to avoid delays during video playback. This algorithm is applied to all frames of the video.

## VI. STRATEGY FOR LOW OVERHEAD AND HIGH POWER SAVING

### A. RELATIONSHIP BETWEEN ESC METHOD AND DECODING PROCESS

When the user begins the video playback, compressed bit streams are called in. The entropy of the bitstreams is decoded according to the data elements, and thus the bitstreams undergo an inverse quantization process. The header data of the bitstreams are used to generate the same predicted

blocks as the original predicted blocks, and the predicted blocks are combined with the inverse quantized information. This information undergoes a filtering process to generate individual decoded blocks. Fig. 12 shows the series of processes applied by a typical H.264 decoder [31]. In this paper, after undergoing the decoding process, the YCbCr information immediately prior to being converted into RGB is used. In the decoding process, the video data are stored as the YCbCr color space in units of macroblocks. When the user plays a video, the YCbCr color space is decompressed and converted into the RGB color space in the buffer. The information in the decompressed the YCbCr color space in one macroblock has the same meaning as the RGB information in the same region. In this paper, a process to calculate the entropy is applied for every frame. The calculation results in the YCbCr color space are quite similar to those in the RGB color space, while reducing the computing overhead.

### B. CONSTRUCTING LOOKUP TABLES

A power model of an AMOLED display is shown through Eq. (4). In this paper, the relationship between the YCbCr information and the characteristics of the power consumption of the display panel was used to minimize the computing overhead while maximally reducing the power consumption. First, the relationship with the RGB-YCbCr color spaces shown in Fig. 13 was used. As can be seen in Fig. 13 and Table 2, individual vertexes of the hexahedron show particular colors, and regularity exists in the distances between the colors.

The power was measured by dividing the Y plane into six planes, excluding the black and white points, out of

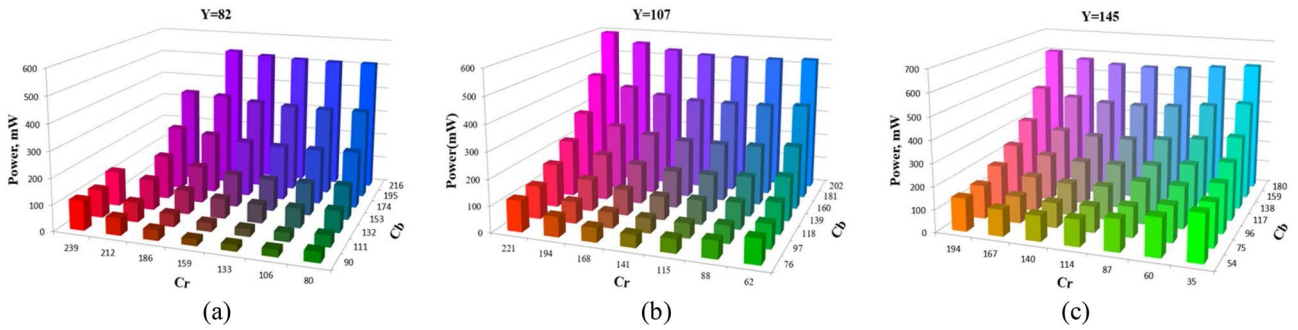


FIGURE 11. Illustrations of the relationship between power consumption and (Cb, Cr) components: (a)  $Y = 82$ , (b)  $Y = 107$ , and (c)  $Y = 145$ .

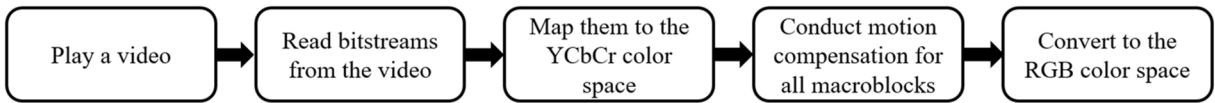


FIGURE 12. Decoding process of a typical H.264 decoder.

TABLE 2. Characteristic points of the YCbCr color space.

Color	White	Yellow	Cyan	Green	Magenta	Red	Blue	Black
R	255	255	0	0	255	255	0	0
G	255	255	255	255	0	0	0	0
B	255	0	255	0	255	0	255	0
Y	235	210	170	145	107	82	41	16
Cb	128	16	166	54	202	90	240	128
Cr	128	146	16	34	222	240	110	128

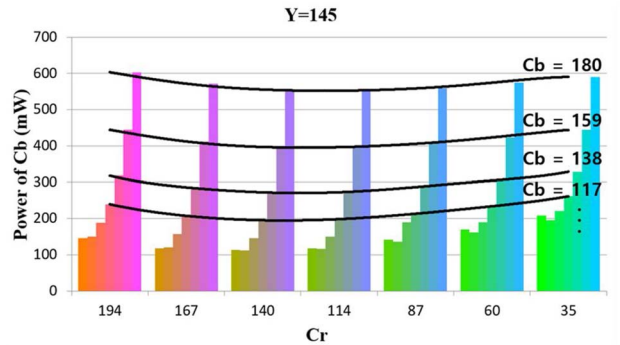


FIGURE 14. Cb, Cr vs. power consumption graph when  $Y = 145$ .

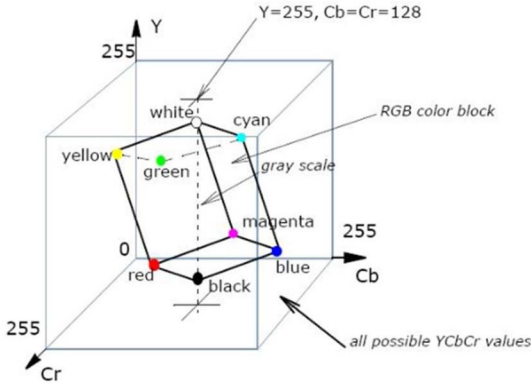


FIGURE 13. RGB-YCbCr color spaces [32].

the eight vertices, and then evenly dividing the individual planes into Cb and Cr. Other sections not measured were sampled based on the measured sections. Fig. 11 shows the power consumption of Cb and Cr for an AMOLED panel when Y in the YCbCr color space was 82, 107, and 145. Fig. 14 shows the power consumption graphs of Cb and Cr when Y was 145. Because the power consumption does not linearly increase when the individual components increase in the case of YCbCr, unlike with RGB, the direction of compensation should be determined. The direction of compensation is determined to minimize the power consumption based on Fig. 14, which is processed into LUT 2 through the ESC-DVS algorithm.

In the RGB color space, as shown through Eq. (4), the power consumption increases as the pixel levels of R, G, and B increase. However, as can be seen from Fig. 14, in the YCbCr color space, changes in power consumption according to Cb, Cr on a fixed Y plane do not follow a general linear graph. To compensate these characteristics quickly in real-time for the board used, a table of the characteristics was created to process the compensation. If multiple candidates for compensation appear during the implementation of the ESC-DVS, as shown in Fig. 14, the compensation will be made toward the point where the least amount of power will be consumed. Although Fig. 14 provides an example regarding the changes in Cb, showing Cr along the horizontal axis, for an actual compensation, the minimum power consumption points are determined by considering both Cb and Cr. As shown in Fig. 8, the voltage is scaled according to Y in the current frame, and Y is compensated following the voltage scaling. Therefore, because Y in the Y-plane is fixed to  $Y'$  during the Cb, Cr component compensations, only the compensations of Cb, Cr are considered. However, Cb, Cr compensations have little effect on the luminance.

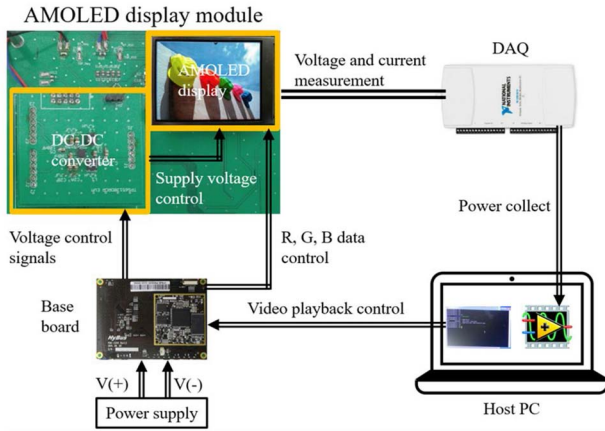


FIGURE 15. Experiment setup.

Fig. 10 shows the LUT application structure along with the ESC-DVS processes. First, LUT 1 shows the relationship between the supply voltage and  $Y$ . The value of  $Y$  is increased to recover the luminance based on the decrease in voltage. Because video distortions may remain in cases in which only the luminance is compensated, the color differences are compensated. Considering the characteristic in which linear relationships are not formed in the YCbCr color space, as shown in Figures 10 and 14, in LUT 2, the direction of compensation is determined. Whether the values should be increased or reduced through compensation should be determined toward a reduction in power consumption. When the direction of compensation has been determined in LUT 2, the actual compensation is made through LUT 3 within the range in which the Euclidean distance does not exceed the JND. To calculate the JND, the optimum condition should be selected through a process to obtain the Euclidean distance after conversions are made from YCbCr into RGB, XYZ, and the CIE Lab color space, which is a burdensome process for real-time video playback. LUTs are used to simplify this process, which is faster than compensating the RGB pixels.

## VII. EXPERIMENTS AND RESULTS

### A. EXPERIMENT SETUP

Fig. 15 shows the environment used, which composed of a board implemented using an AMOLED display for the proposed ESC-DVS algorithm. To supply voltage, the experimental environment was set up by connecting a Texas Instruments TPS65138 AMOLED DC-DC converter IC [33] to a CHIMEI C0240QGLA-T display module [28]. The resolution of the display module is 240x320 and the color pixel array of the module is the same. In addition, the active area of the module is 36.82 mm x 48.96mm, the outline area of the module is 42mm x 58.6mm, and the diagonal size is 2.4 inch. A National Instruments USB-6210 DAQ [34] and LabView were used for the power measurements. Mplayer, which is an open-software player for Linux, was used for video playback. The information on the videos used in these experiments is shown in Table 3. To conduct the testing

TABLE 3. Test videos used in the experiments.

	Type	Duration	No. of frames	Codec
Test video 1	News [35]	1 m 11 s	1709	H.264
Test video 2	Sports [36]	3 m 35 s	5162	H.264
Test video 3	Movie [37]	2 m 26 s	3518	H.264
Test video 4	Entertainment [38]	2 m 17 s	3290	H.264
Test video 5	Cartoon [16]	1 m 48 s	2595	H.264
Test video 6	Video game [16]	2 m 49 s	4062	H.264
Test video 7	Movie [16]	1 m 23 s	1994	H.264

TABLE 4. Recall and precision for test videos.

	Recall (ESC-DVS)	Precision (ESC-DVS)	Recall [16]	Precision [16]
Test video 1	1	0.7	0.6	0.55
Test video 2	1	0.89	0.46	0.63
Test video 3	0.90	0.84	0.85	0.37
Test video 4	0.96	0.82	0.78	0.54
Test video 5	0.95	0.74	0.88	0.61
Test video 6	1	0.14	0.71	0.07
Test video 7	0.91	0.79	0.90	0.51
Average	0.94	0.69	0.80	0.40

with diverse types of videos, the authors selected a news program, sports highlights, a movie trailer, and an entertainment program. In addition, for comparison, the experiments were also conducted with videos used in a previous study on a different technique [16]. Among the videos used in the previous study, only the news video could not be obtained and was unavoidably excluded from the experiments.

### B. EXPERIMENT RESULTS

#### B.1. RESULTS OF SCENE CHANGE DETECTION

Table 4 shows the results of the scene change detection from the test videos based on the recall and precision shown through Eq. (5) and (6). The recall refers to the ratio of experimental results indicating true values to the actual true values, and precision refers to the ratio of actual true values to the experimental results indicating true values. These two terms are frequently used as scales of experimental indicators in the areas of pattern recognition and information searches [39].

$$\text{Recall} = \frac{N_{\text{boundaries detected}}}{N_{\text{true boundaries}}} \quad (5)$$

$$\text{Precision} = \frac{N_{\text{true boundaries detected}}}{N_{\text{boundaries detected}}} \quad (6)$$

**TABLE 5. Recall and precision for test videos in abrupt scene change.**

	Recall (ESC-DVS)	Precision (ESC-DVS)	Recall [16]	Precision [16]
Test video 1	1	0.8	0.5	0.67
Test video 2	1	0.89	0.51	0.81
Test video 3	0.93	0.85	0.92	0.85
Test video 4	0.96	0.85	0.84	0.8
Test video 5	0.96	0.75	0.92	0.75
Test video 6	-	-	-	-
Test video 7	0.90	0.79	0.94	0.80
Average	0.95	0.68	0.85	0.60

Table 4 shows the results of the scene change detection from the videos shown in Table 3 using ESC-DVS and the previous technique [15]. The detection rates of ESC-DVS were shown to be higher than those of the existing technique. First, the recall results by ESC-DVS were shown to be somewhat poorer for test video 3 because this particular video has more gradual scene change effects, such as fade-outs, compared to the other videos, and because its entropy changes are frequent owing to its characteristic as a preview of other content. The precision results by ESC-DVS were shown to be remarkably low for test video 6 because videos based on a first-person view such as games have a characteristic of similarity owing to the fact that they successively continue regardless of any changes in entropy. Because scene changes can be more accurately detected if the threshold values of the individual test videos are optimized, studies for variably setting the entropy thresholds according to the video information are also necessary.

Although the existing technique detects abrupt scene changes relatively well, in the case of gradual scene changes, it detected a single scene change effect different many times. In particular, the precision results decreased as the number of frames containing a scene change effects increased. This is attributable to the characteristics of the existing technique, which divides each frame into 16 regions and detects any changes only when the majority of the regions have been changed so that scene changes without any change in the color differences between the background and the object. In the proposed ESC-DVS algorithm, to reduce the number of errors, detection is deferred until the changes in entropy in the scene change effect are converged at a certain value.

For comparison, the results of the scene change detection shown in Table 4 were divided into Tables 5 and 6 based on whether the changes were abrupt or gradual scene change effects. First, Table 5 shows the results of abrupt scene change detection from the test videos. Although most of the recall and precision results by ESC-DVS show higher detection rates compared to the existing technique, this was not the case for test video 7 because the existing technique

**TABLE 6. Recall and precision for test videos in gradual scene change.**

	Recall (ESC-DVS)	Precision (ESC-DVS)	Recall [16]	Precision [16]
Test video 1	1	0.6	0.67	0.5
Test video 2	1	0.86	0.17	0.11
Test video 3	0.82	0.77	0.54	0.07
Test video 4	0.92	0.69	0.5	0.15
Test video 5	0.83	0.63	0.33	0.09
Test video 6	1	0.14	0.71	0.07
Test video 7	1	0.75	0.33	0.03
Average	0.88	0.73	0.47	0.09

**TABLE 7. Average power saving for the test videos.**

	Power saving (%)
Test video1	18.17
Test video2	14.79
Test video3	19.44
Test video4	26.64
Test video5	21.51
Test video6	18.32
Test video7	30.27
Average	21.31

shows a high detection rate in cases where the pixel differences between the scene boundary frame and the previous frame are clear, such as in a movie preview. Existing studies have a problem of being unable to accurately detect scene changes with unclear pixel changes or with pixel changes in less than half of the regions, and therefore the detection rates of the ESC-DVS algorithm are higher. Because ESC-DVS is based on changes in pixel distribution obtained through entropy, it shows higher accuracy rates than detection based on simple pixel differences. There are no measured values for test video 6 because it has no abrupt scene changes.

## B.2. POWER SAVING

Table 7 shows the average power saving ratios of ESC-DVS for the test videos. Among the test videos, test video 7, which has relatively brighter frames, showed the highest power saving ratio, whereas test video 3, consisting of the darkest frames, showed the lowest power saving ratio. When the frames are brighter, a large amount of power saving can be achieved with only a small voltage scaling.

Fig. 16 and 17 show the relationship between the Y component in the YCbCr color space and the power consumption of the display panel during the playback of test videos 1 and 6, respectively. In these figures, it can be seen that the power consumption is greatly affected by the Y components of the macroblocks in each frame. As the videos gradually become brighter, the Y components of the macroblocks also increase, leading to increases in pixel size and power consumption. In the case of bright scenes, although the



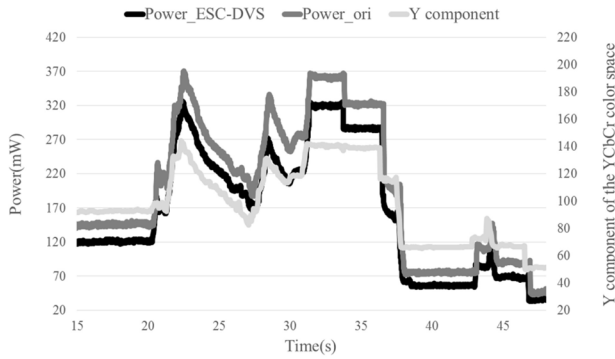


FIGURE 16. Power consumption and Y component for test video 1.

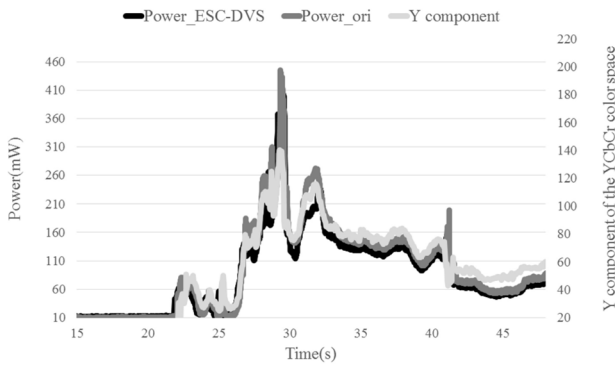


FIGURE 17. Power consumption and Y component for test video 6.

voltage drops are smaller compared to dark scenes, the power saving is larger than in dark scenes because the amount of power consumed by the original video is greater.

In Fig. 16 and 17, the black line shows the power consumption of the ESC-DVS, the dark-gray line indicates the power consumption of the original video, and the light-gray line is the average Y of the YCbCr color space in each frame. In Fig. 16, the dark-gray and black lines mostly change similarly with the changes in the light-gray line. In other word, the black and dark-gray lines change in accordance with the changes in the light-gray line. However, at around 33 s, large power changes occur rapidly despite the slight change in the light-gray line, which indicates that the changes in Y do not have an absolute effect. Fig. 17 shows almost no differences between the dark-gray and black lines before the first-person view is continued with a few scene changes, and therefore without voltage scaling.

### B.3. VIDEO QUALITY ON AN AMOLED DISPLAY PANEL

Fig. 18 compares the changes in power consumption and luminance of the original video, voltage scaling without compensation, and the application of ESC-DVS for test videos 1 through 7. The screenshots in Fig. 18 were taken of the panel under various conditions. Because the experiments in this paper were conducted on a board implemented with an actual AMOLED display, the quality was checked based on changes in the Euclidean distances and luminance, and it was identified that the quality of ESC-DVS did not differ

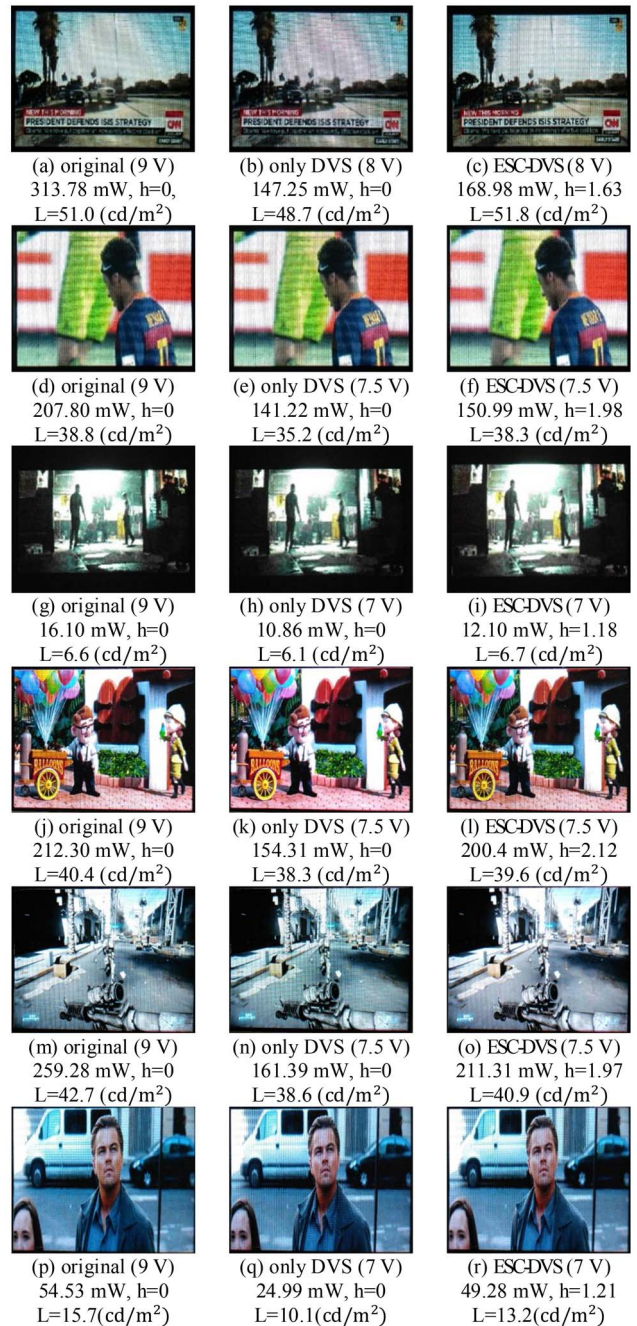


FIGURE 18. Comparison of visual satisfaction for original (9V), voltage scaling without compensation, and ESC-DVS method.

when compared to the original video. In the case of test video 1, although a loss of luminance of 4.51% occurred between (a) the original video and (b) when voltage scaling only was applied without compensation, (c) the ESC-DVS algorithm resulted in a luminance loss of 1.57%, indicating that 65.19% of the loss was recovered. In the case of test video 6, whereas a luminance loss of 9.6% occurred between (m) and (n), a luminance loss of 4.22 % occurred between (m) and (o), indicating that 56.04% of the loss was recovered.

The ESC-DVS recorded less power saving than cases where only voltage scaling was applied without compensation because the ESC-DVS compensated the pixel changes owing to the voltage scaling. However, it achieved a large power saving while maintaining the quality when compared to the original video. In the case of test video 1, the power consumption was reduced by 46.15% between (a) and (c), and in the case of test video 6, the power consumption was reduced by 18.5% between (m) and (o). Because voltage scaling and pixel compensation were applied within a range not exceeding the JND, most of the test videos do not differ significantly from the original versions. In cases in which only voltage scaling was applied without compensation, distortion phenomena may have occurred in certain cases, resulting in darker videos compared to the original following the frame changes, as was the case with (b) and (n). If the process to compensate the three components, Y, Cb, and Cr, is implemented, the quality can be recovered to closer to that of the original video than in cases when only voltage scaling was applied. In addition, a large power saving can be achieved, as shown in Fig. 8.

#### B.4. TIME ANALYSIS

Because the ESC-DVS algorithm proposed in this paper is executed on a board implemented using an AMOLED display, operating in real-time is very important. Existing techniques that use entropy [12], [13] calculate the gray level of all of the pixels, and thus the entropy using the results of this calculation. However, for the ESC-DVS algorithm, only the entropy is calculated without any process for separately calculating the Y component because the Y components of the macroblocks are used in the decoding process. Because one macroblock consists of 256 pixels, and four Y components are generated per macroblock during decoding, arithmetically, the computing overhead of the entropy calculation process can be reduced to 1/64, and if the process used to calculate the gray level in the RGB color space is included, a larger reduction in the computing overhead may be achieved. The approaches in [12] and [13] cause serious overhead for video playback on experimental boards because mutual information or the SURF features are included together with the entropy calculation process. Accordingly, the execution time was compared using the scene change detection technique in [15], which has relatively low overhead. The execution times were compared on a real board for the test videos, and according to the results, the ESC-DVS algorithm runs 84-times faster compared with the existing technique. When measured using the seven test videos, where the existing technique took 11.8 ms on average, the ESC-DVS algorithm took only 0.14 ms. Given that popularly used videos are mainly played at 30 or 24 fps, the technique used should be executed within a maximum of 33.3 or 41.7 ms per frame, respectively. The computing overhead of the ESC-DVS algorithm was identified as 0.42% and 0.34% for these frame rates, respectively, as described in Table 8.

TABLE 8. Average elapsed time per frame for test videos (ms).

Original (24 fps)	Original (30 fps)	[16]	ESC-DVS
41.67	33.33	11.80	0.14

#### VIII. DISCUSSION

In this paper, we proposed a novel DVS algorithm using entropy-based scene change detection for mobile AMOLED displays. The ESC-DVS algorithm showed a good level of performance while reducing the computing overhead compared to an existing technique. The authors tried to solve the problems of existing studies, and herein discuss different directions for future work.

The ESC algorithm cannot detect all transition effects in all videos. Such a technique does not yet exist, and related techniques are being improved through various studies. For more accurate detection, first, the threshold used to detect scene changes during video playback can be actively changed. In this paper, the threshold was fixed at the experimentally obtained value. Because an infinite number of transition effects can be made by an editor, understanding the frame change characteristics is of utmost importance, and actively changed thresholds will be a key to more accurate detection than that achieved by existing studies.

Owing to the recent developments of related technologies, discussions regarding next-generation video formats are at their peak. Currently, video formats are in a transitional period, and will be changed from the H.264 format to the H.265 format. The H.265 format has an advantage in reducing the file size by half compared to H.264 for the same picture quality. However, it has a shortcoming of consuming 1.2- to 2-times more resources during encoding/decoding compared to H.264 owing to its complicated compression algorithm [40]. The ESC-DVS algorithm can be sufficiently applied to H.265 because it provides weight to the macroblock sizes to calculate the entropy.

As the results in Table 4 show, poor scene change detection is obtained from videos with a first-person view because a single scene continues uninterrupted for a lengthy period of time in such videos. Because the purposes of this paper are power saving and maintaining the same video quality as the original version, techniques applied based on the content shown are necessary for such videos. This remains as future work, however.

The parts in a mobile device that consume the largest amount of power are the display panel and CPU/GPU. Studies on controlling the CPU/GPU voltage and thereby reducing the power consumption have been steadily conducted. Although this paper does not address the relevance of the content being displayed because it is aimed at power saving for mobile AMOLED displays, in future work, we will combine these two techniques.

## IX. CONCLUSION

In this paper, we proposed a novel DVS algorithm called ESC-DVS for mobile AMOLED displays. It minimizes the computing overhead by processing the scene change detection in macroblock units using the entropy values for Y, Cb, and Cr components. ESC-DVS was implemented based on the degree of human vision satisfaction, and its compensation was realized in the direction required to recover the losses that occur during voltage scaling. In addition, when color difference components are compensated, the compensation is fulfilled in the direction toward the maximization of power saving within the range of the JND when considering the panel characteristics. Consequently, the proposed technique achieved a power saving of 21.31% on average while showing better scene detection results compared to a previous DVS technique. ESC-DVS runs 84-times faster at maximum than the previous technique.

## REFERENCES

- [1] CNN. (2016). *Apple Could Be Radically Redesigning the iPhone*. Accessed on Dec. 2016. [Online]. Available: <http://money.cnn.com/2016/03/28/technology/new-iphone/>
- [2] N. T. Kalyani and S. J. Dhoble, "Organic light emitting diodes: Energy saving lighting technology—A review," *Renew. Sustain. Energy Rev.*, vol. 16, no. 5, pp. 2696–2723, Jun. 2012.
- [3] C. Yoon, D. Kim, W. Jung, C. Kang, and H. Cha, "AppScope: Application energy metering framework for android smartphones using kernel activity monitoring," in *Proc. USENIZ ATC*, Boston, MA, USA, Jun. 2012, pp. 387–400.
- [4] L. Zhang *et al.*, "Accurate online power estimation and automatic battery behavior based power model generation for smartphones," in *Proc. IEEE CODES/ISSS*, Scottsdale, AZ, USA, Oct. 2010, pp. 105–114.
- [5] A. Carroll and G. Heiser, "An analysis of power consumption in a smartphone," in *Proc. USENIX*, Boston, MA, USA, Jun. 2010, p. 21.
- [6] Computer world. (2015). *App Usage—Smartphones Versus Tablets*. Accessed on Dec. 2016. [Online]. Available: <http://www.computerworld.com/article/2861436/app-usage-smartphones-versus-tablets.html>
- [7] W. Hu, N. Xie, L. Li, X. Zeng, and S. Maybank, "A survey on visual content-based video indexing and retrieval," *IEEE Trans. Syst., Man, Cybern. C, Appl. Rev.*, vol. 41, no. 6, pp. 797–819, Nov. 2011.
- [8] D. Lelescu and D. Schonfeld, "Statistical sequential analysis for real-time video scene change detection on compressed multimedia bitstream," *IEEE Trans. Multimedia*, vol. 5, no. 1, pp. 106–117, Mar. 2003.
- [9] P. Panchal, S. Merchant, and N. Patel, "Scene detection and retrieval of video using motion vector and occurrence rate of shot boundaries," in *Proc. IEEE NUICON*, Ahmedabad, India, Dec. 2012, pp. 1–6.
- [10] C.-L. Huang and B.-Y. Liao, "A robust scene-change detection method for video segmentation," *IEEE Trans. Circuits Syst. Video Technol.*, vol. 11, no. 12, pp. 1281–1288, Dec. 2001.
- [11] X. Yi and N. Ling, "Fast pixel-based video scene change detection," in *Proc. IEEE ISCAS*, Kobe, Japan, May 2005, pp. 3443–3446.
- [12] C.-G. Liu and S. Wang, "An adapting to light change pixel layer based background model for moving objects detection in a dynamic scene," in *Proc. DCABES*, Guilin, China, Oct. 2012, pp. 405–408.
- [13] Z. Cemekova, I. Pitas, and C. Nikou, "Information theory-based shot cut/fade detection and video summarization," *IEEE Trans. Circuits Syst. Video Technol.*, vol. 16, no. 1, pp. 82–91, Jan. 2006.
- [14] J. Baber, N. Afzulpurkar, M. N. Dailey, and M. Bakhtyar, "Shot boundary detection from videos using entropy and local descriptor," in *Proc. IEEE DSP*, Jul. 2011, pp. 1–6.
- [15] D. Shin, Y. Kim, N. Chang, and M. Pedram, "Dynamic voltage scaling of OLED displays," in *Proc. IEEE DAC*, San Diego, CA, USA, Jun. 2011, pp. 53–58.
- [16] X. Chen, J. Zeng, Y. Chen, M. Zhao, and C. J. Xue, "Quality-retaining OLED dynamic voltage scaling for video streaming applications on mobile devices," in *Proc. IEEE DAC*, San Francisco, CA, USA, Jun. 2012, pp. 1000–1005.
- [17] C.-H. Lin, C.-K. Kang, and P.-C. Hsiu, "Catch your attention: Quality-retaining power saving on mobile OLED displays," in *Proc. IEEE DAC*, San Francisco, CA, USA, Jun. 2014, pp. 1–6.
- [18] X. Chen, Y. Chen, and C. J. Xue, "DaTuM: Dynamic tone mapping technique for OLED display power saving based on video classification," in *Proc. IEEE DAC*, San Francisco, CA, USA, Jun. 2015, pp. 1–6.
- [19] T.-C. Chang and S. S.-D. Xu, "Real-time quality-on-demand energy-saving schemes for OLED-based displays," in *Proc. IEEE ISIE*, Taipei, Taiwan, May 2013, pp. 1–5.
- [20] S. Kim, S. Hyun, T. Heo, D. Im, and J. Huh, "Blind: Power saving color transform method for OLED displays," in *Proc. IEEE ICCE*, Las Vegas, NV, USA, Jan. 2016, pp. 500–501.
- [21] Y. Tan, P. Malani, Q. Qiu, and Q. Wu, "Workload prediction and dynamic voltage scaling for MPEG decoding," in *Proc. IEEE DAC*, Yokohama, Japan, Jan. 2006, pp. 911–916.
- [22] J.-Y. Hwang, S.-B. Suh, W.-B. Yi, J.-H. Kim, and J.-H. Kim, "Low power MPEG4 player," in *Proc. Linux Symp.*, Ottawa, ON, Canada, Jul. 2008, pp. 219–227.
- [23] C.-C. Ku and T.-M. Wang, "Luminance-based adaptive color saturation adjustment," *IEEE Trans. Consum. Electron.*, vol. 51, no. 3, pp. 939–946, Aug. 2005.
- [24] J.-S. Chiang, C.-H. Hsia, H.-W. Peng, C.-H. Lien, and H.-T. Li, "Saturation adjustment method based on human vision with YCbCr color model characteristics and luminance changes," in *Proc. IEEE ISPACS*, Taipei, Taiwan, Nov. 2012, pp. 136–141.
- [25] M. Park and M. Song, "Saving power in video playback on OLED displays by acceptable changes to perceived brightness," *J. Display Technol.*, vol. 12, no. 5, pp. 483–490, May 2016.
- [26] K. Jack, *YCbCr to RGB Considerations*, Intersil, Milpitas, CA, USA, 1997, pp. 1–4.
- [27] A. Bartolini, M. Ruggiero, and L. Benini, "HVS-DBS: Human visual system-aware dynamic luminance backlight scaling for video streaming applications," in *Proc. ACM EMSOFT*, Oct. 2009, pp. 21–28.
- [28] *TPS65138: Dual Output AMOLED Display Power Supply Datasheet*. Texas Instrum., Dallas, TX, USA, 2013. [Online]. Available: <http://www.ti.com/lit/ds/symlink/tps65138.pdf>
- [29] G. Sharma and R. Bala, *Digital Color Imaging Handbook*. Boca Raton, FL, USA: CRC Press, Dec. 2002, pp. 30–32.
- [30] M. Dong, Y.-S. K. Choi, and L. Zhong, "Power modeling of graphical user interfaces on OLED displays," in *Proc. IEEE DAC*, San Francisco, CA, USA, Jul. 2009, pp. 911–916.
- [31] I. E. G. Richardson, *H.264 and MPEG-4 Video Compression: Video Coding for Next-Generation Multimedia*. Chichester, U.K.: Wiley, 2004, pp. 28–41.
- [32] Intel. *RGB Colors Cube in the YCbCr Space*. Accessed on Nov. 2016. [Online]. Available: <https://software.intel.com/en-us/node/503873#FIG6-5>
- [33] C0240QGLA-T: Approval Product Specification. CHIMEI, Tainan, Taiwan, 2008. [Online]. Available: <http://html.alldatasheet.com/html-pdf/317814/AZDISPLAYS/C0240QGLA-T/604/1/C0240QGLA-T.html>
- [34] DAQ: USB-6210. Nat. Instrum., Austin, TX, USA. [Online]. Available: <http://sine.ni.com/nips/cds/view/p/lang/en/nid/203223>
- [35] CNN. (2015). *Obama Challenges Media on ISIS Coverage*. Accessed on Nov. 2016. [Online]. Available: <https://www.youtube.com/watch?v=asRJLDneVqg>
- [36] FIFATV. (2015). *Final Highlights: River Plate vs Barcelona*. Accessed on Nov. 2016. [Online]. Available: <https://www.youtube.com/watch?v=1NRtg2rQH7s>
- [37] Marvel Entertainment. (2015). *Marvel's Captain America: Civil War*. Accessed on Nov. 2016. [Online]. Available: <https://www.youtube.com/watch?v=43NWzay3W4s>
- [38] DIVX. *Micayala Gatto*. Accessed on Nov. 2016. [Online]. Available: <http://www.divx.com/en/devices/profiles/video>
- [39] M. Buckland and F. Gey, "The relationship between recall and precision," *J. Amer. Soc. Inf. Sci.*, vol. 45, no. 1, pp. 12–19, Jan. 1994.



- [40] J. R. Ohm, G. J. Sullivan, H. Schwarz, T. K. Tan, and T. Wiegand, "Comparison of the coding efficiency of video coding standards—Including high efficiency video coding (HEVC)," *IEEE Trans. Circuits Syst. Video Technol.*, vol. 22, no. 12, pp. 1669–1684, Dec. 2012.
- [41] B.-H. Lee and Y.-J. Kim, "Dynamic voltage scaling using scene change detection for video playback on mobile AMOLED displays," in *Proc. IEEE ISLPED*, San Francisco, CA, USA, Aug. 2016, pp. 302–307.



**BYUNG-HOON LEE** received the B.S. degree from the Department of Electrical and Computer Engineering, Ajou University, Suwon, South Korea, in 2015, where he is currently pursuing the master's degree. His research interests include embedded systems and software, display system, and power measurement and analysis.



**YOUNG-JIN KIM** (S'05–M'08) received the B.S. and M.S. degrees in electrical engineering and the Ph.D. degree in computer science and engineering from Seoul National University, Seoul, South Korea, in 1997, 1999, and 2008, respectively. From 1999 to 2003, he was with the Electronics and Telecommunications Research Institute, Daejeon, South Korea. He was an Assistant Professor with the Department of Computer Science and Engineering, Sun Moon University, Asan, South Korea, from 2008 to 2011. He is currently an Associate Professor with the Department of Electrical and Computer Engineering, Ajou University, Suwon, South Korea. His current research interests include embedded systems and software, display systems and image processing, mobile storage systems, and low-power technology.